frontiers | Frontiers in Endocrinology

TYPE Original Research
PUBLISHED 20 March 2023
DOI 10.3389/fendo.2023.1135973

OPEN ACCESS

EDITED BY
Kun Li,
Hangzhou Medical College, China

REVIEWED BY
Lucia Rocco,
University of Campania Luigi Vanvitelli, Italy
Miguel Betancourt,
Metropolitan Autonomous University, Mexico

*CORRESPONDENCE
Philip C. N. Chiu
pchiucn@hku.hk
Jian-Ping Ou
oujp3@mail.sysu.edu.cn

SPECIALTY SECTION
This article was submitted to Reproduction, a section of the journal Frontiers in Endocrinology

RECEIVED 02 January 2023
ACCEPTED 07 March 2023
PUBLISHED 20 March 2023

CITATION
Leung ETY, Lee BKM, Lee C-L, Tian X, Lam KKW, Li RHW, Ng EHY, Yeung WSB, Ou J-P and Chiu PCN (2023) The role of spermatozoa-zona pellucida interaction in selecting fertilization-competent spermatozoa in humans.
Front. Endocrinol. 14:1135973.
doi: 10.3389/fendo.2023.1135973

The role of spermatozoa-zona pellucida interaction in selecting fertilization-competent spermatozoa in humans

Erica T. Y. Leung[1], Brayden K. M. Lee[1], Cheuk-Lun Lee[1,2], Xinyi Tian[1], Kevin K. W. Lam[1,2], Raymond H. W. Li[1,2], Ernest H. Y. Ng[1,2], William S. B. Yeung[2], Jian-Ping Ou[1,3]* and Philip C. N. Chiu[1,2]*

[1]Department of Obstetrics and Gynaecology, Li Ka Shing Faculty of Medicine, The University of Hong Kong, Hong Kong, Hong Kong SAR, China, [2]Shenzhen Key Laboratory of Fertility Regulation, The University of Hong Kong – Shenzhen Hospital, Shenzhen, China, [3]Center for Reproductive Medicine, The Third Affiliated Hospital, Sun Yat-sen University, Guangzhou, China

Human fertilization begins when a capacitated spermatozoon binds to the zona pellucida (ZP) surrounding a mature oocyte. Defective spermatozoa-ZP interaction contributes to male infertility and is a leading cause of reduced fertilization rates in assisted reproduction treatments (ARTs). Human ejaculate contains millions of spermatozoa with varying degrees of fertilization potential and genetic quality, of which only thousands of motile spermatozoa can bind to the ZP at the fertilization site. This observation suggests that human ZP selectively interacts with competitively superior spermatozoa characterized by high fertilizing capability and genetic integrity. However, direct evidence for ZP-mediated sperm selection process is lacking. This study aims to demonstrate that spermatozoa-ZP interaction represents a crucial step in selecting fertilization-competent spermatozoa in humans. ZP-bound and unbound spermatozoa were respectively collected by a spermatozoa-ZP coincubation assay. The time-course data demonstrated that ZP interacted with a small proportion of motile spermatozoa. Heat shock 70 kDa protein 2 (HSPA2) and sperm acrosome associated 3 (SPACA 3) are two protein markers associated with the sperm ZP-binding ability. Immunofluorescent staining indicated that the ZP-bound spermatozoa had significantly higher expression levels of HSPA2 and SPACA3 than the unbound spermatozoa. ZP-bound spermatozoa had a significantly higher level of normal morphology, DNA integrity, chromatin integrity, protamination and global methylation when compared to the unbound spermatozoa. The results validated the possibility of applying spermatozoa-ZP interaction to select fertilization-competent spermatozoa in ART. This highly selective interaction might also provide diagnostic information regarding the fertilization potential and genetic qualities of spermatozoa independent of those derived from the standard semen analysis.

KEYWORDS

zona pellucida, human spermatozoa, sperm selection, DNA integrity, methylation, protamination, HSPA2, SPACA3

1 Introduction

Infertility is a public health concern affecting approximately 15% of reproductive-aged couples worldwide (1). Assisted reproduction technologies (ARTs) including *in vitro* fertilization (IVF), intrauterine insemination (IUI), intracytoplasmic sperm injection (ICSI) are provided to infertile couples who wish to conceive. Despite major technological advancements, the live birth rate following ART is only about 30% (2).

Sperm quality is a major factor contributing to fertilization success following ARTs (3, 4). During migration through the female reproductive tract, only the fertilization-competent spermatozoa survive the natural selection mechanisms involving anatomical, biochemical, and physiological barriers in a highly specialized microenvironment (5). In ART, the motile and morphologically normal spermatozoa are routinely isolated by either the swim-up or density gradient centrifugation (DGC) according to their motility and density, respectively for subsequent procedures. However, these two surrogate markers lack the discriminatory power to select high-quality spermatozoa according to their fertilization potential and genetic quality (5–10).

Advanced sperm selection methods have been developed to enrich high-quality spermatozoa aiming to improve the fertilization and clinical outcomes (11–14). Two approaches are being used to develop sperm selection methods. One approach is to focus on the intrinsic properties of spermatozoa, such as surface charges and apoptotic status of spermatozoa (15, 16). Another approach is to replicate the natural selection mechanisms such as thermotactic and chemotactic responses in a controlled environment to isolate fertilization-competent spermatozoa in a manner similar to those observed in the female reproductive tract (5, 17, 18). However, contradicting results have been reported on the clinical significance of these methods on ART outcomes (5). In addition, many of these new techniques are small-scaled, which can only process a small volume of sample per run (5). These findings highlight the need for new approaches to sperm selection in ART.

In the fallopian tubes, the capacitated spermatozoa bind to the zona pellucida (ZP) surrounding the released oocyte and undergo acrosome reaction which facilitates the subsequent penetration process for gamete fusion. Defective sperm-ZP binding (DSZPB) is a leading cause of male-factor infertility and fertilization failure in IVF (19–22). Spermatozoa-ZP binding is a highly species specific event that occurs when the specific ligands on the ZP are recognized by the protein receptors located on the capacitated spermatozoa (23). The receptor(s) are multimeric protein complex(es) assembled during capacitation (24). Fertile male ejaculate contains millions of spermatozoa, of which only 14% of the motile spermatozoa are capable of binding to the ZP (25) and only 48% of the ZP-bound spermatozoa can then undergo ZP-induced acrosome reaction (26). These observations suggest that human ZP selectively interacts with high-quality spermatozoa possessing superior genetic integrity and fertilizing capability. However, direct evidence for the existence of this ZP-mediated sperm selection process in humans is lacking. Therefore, the objective of this study is to validate the functional role of human ZP in selecting fertilization-competent spermatozoa.

2 Materials and methods

2.1 Semen and oocyte collection

The research protocol of this study was approved by the Institutional Review Board of the University of Hong Kong/Hospital Authority Hong Kong West Cluster. Semen samples were collected from men attending the Family Planning Association of Hong Kong for premarital checkup after obtaining informed written consent. The residual portion after the routine test was collected for research use. Normal semen samples were selected for research use according to the World Health Organization (WHO) criteria, fifth edition (27): total volume > 1.5 mL, total motility > 40%, progressive motility > 32%, total sperm number > 39×10^6 per ejaculate, concentration > 15×10^6/mL, and viability > 58%, normal morphology > 4%. Direct swim-up method was used to isolate motile and viable spermatozoa from the seminal plasma. In this method, 1.0 mL of thoroughly mixed semen was overlaid by 1.5 mL of Earle Balanced Salt Solution (EBSS; Flow Laboratories, Irvine, United Kingdom) supplemented with 0.3% bovine serum albumin (BSA), 0.3 mmol/l sodium pyruvate, 0.16 mmol/L penicillin G, 0.05 mmol/l streptomycin sulfate, and 14 mmol/L sodium bicarbonate (all from Sigma, MO, USA) (EBSS/0.3% BSA). The tube was then placed at a 45° angle and incubated at 37°C with 5% CO_2 for one hour to allow motile spermatozoa to migrate from the seminal plasma into the overlaying medium. 1 mL of the top layer of the medium was collected, transferred into a sterile 15 mL centrifuge tube, and centrifuged at 500g for 5 min twice. The washed pellet was then resuspended with EBSS/0.3% BSA and diluted to the appropriate concentrations (1×10^6 or 2×10^6 spermatozoa/ml). All processed spermatozoa were incubated in EBSS supplemented with 3% BSA (EBSS/3%BSA) to induce capacitation for the spermatozoa-ZP coincubation assays (28).

Oocytes were collected from infertile women attending IVF treatment at the Queen Mary Hospital, Hong Kong. Immature oocytes (germinal vesicle/metaphase I oocytes) or mature metaphase II oocytes that failed to achieve fertilization following conventional insemination were donated from patients with informed consent and stored in high-salt oocyte storage buffer containing 1.5 M $MgCl_2$, 0.1% polyvinyl pyrrolidone (PVP) and 40 mM HEPES with pH 7.2. Morphologically abnormal oocytes were discarded.

2.2 Evaluation of sperm motility

Sperm motility was assessed by the computer-assisted sperm analysis (CASA) system (CEROS system, Hamilton Thorne, MA, USA). For each measurement, 10 µL of sperm sample was transferred on a glass slide (Hamilton Thorne, USA) specifically made for the CASA system equipped with a warmed stage at 37°C. A minimum of 200 spermatozoa per sample in randomly selected fields were examined to analyze the following sperm motion parameters: 1) Progressive motility (%), 2) average path velocity (VAP, µm/s), 3) straight line velocity (VSL; µm/s), 4) curvilinear

velocity (VCL, μm/s), 5) lateral amplitude (μm), 6) beat frequency (Hz), 7) straightness (%), 8) linearity (%), 9) elongation of sperm head (%), and 10) area (μm).

2.3 Evaluation of sperm viability

Sperm viability was assessed by the trypan blue exclusion assay. Spermatozoa were thoroughly mixed with an equal volume of trypan blue dye (1:1 ratio) on a sterile glass slide and kept at 37°C for 5 min prior to examination. The mixture was then evaluated under a light microscope with a magnification of 400x. Viable spermatozoa appeared transparent whilst non-viable spermatozoa with disrupted plasma membranes were stained blue. A minimum of 200 spermatozoa per sample in randomly selected fields were quantified to determine the overall viability.

2.4 ZP-bound spermatozoa collection

ZP-bound spermatozoa were collected by a modified spermatozoa-ZP coincubation assay (25). In brief, 4 human oocytes were transferred into a 30 μL droplet of EBSS/3% BSA containing 2×10^6 spermatozoa covered with mineral oil for coincubation at 37°C in 5% CO_2 for 30 min unless stated otherwise. After incubation, the oocytes were successively washed with 3 droplets of EBSS/no BSA to dislodge loosely bound spermatozoa. The ZP-bound spermatozoa were then removed from the surface of the oocytes through vigorous aspiration using a glass pipette in a confined area containing 10 μL of EBSS/no BSA on a sterile glass slide for further analysis.

2.5 ZP-unbound spermatozoa collection

ZP-unbound spermatozoa were collected by a modified continuous spermatozoa-ZP coincubation assay (25). In this method, 4 human oocytes were transferred into a 20 μL droplet of EBSS/3%BSA containing 1×10^6 spermatozoa for a 6-h incubation at 37°C in 5% CO_2. The following procedures were performed at intervals of 2, 4 and 6 h. The oocytes were successively washed with 3 droplets of EBSS/no BSA to dislodge any loosely bound spermatozoa and transferred into a fresh droplet of EBSS/no BSA for observation under a light microscope. Only spermatozoa tightly bound to the ZP with their sperm heads were quantified whilst those bound to the ZP with their tails, or any other regions were omitted. The ZP-bound spermatozoa were then removed from the ZP as described above and the oocytes were transferred back into the original sperm droplet for further coincubation. All spermatozoa remaining in the sperm droplet after 6 h of coincubation were considered as unbound spermatozoa, which were subsequently collected for further analysis.

2.6 Evaluation of the acrosomal status of spermatozoa

The acrosomal status of spermatozoa was evaluated by the fluorescein isothiocyanate conjugated *Pisum sativum* (FITC-PSA) (Sigma) staining. 20 μL of ZP-bound and unbound spermatozoa were allowed to air-dry in a small area on a sterile glass slide at 37°C. The slide was then washed with distilled water thrice. The spermatozoa were incubated with 50 μL of FITC-PSA (20 μg/mL) for 1 h at 37°C in the dark. The slides were rinsed with distilled water twice and mounted with DAKO mounting solution (Dako, CA, USA). The stained spermatozoa were observed under a fluorescence microscope (Zeiss, Oberkochen, Germany) at a magnification of 600x using excitation/emission wavelengths of 495 nm/515 nm. Acrosome-intact spermatozoa were stained with bright green, fluorescent signals in no less than half of the acrosomal regions whilst acrosome-reacted spermatozoa only had fluorescent signals at the equatorial region or completely lacked fluorescent signals in the acrosomal region. A minimum of 100 spermatozoa/sample was quantified to determine the acrosome reaction rates.

2.7 Immunodetection of protein expressions on spermatozoa

Capacitated sperm suspensions were fixed with 0.4% paraformaldehyde for 10 min and washed with EBSS/no BSA twice. The fixed spermatozoa were individually incubated with the primary antibodies against heat shock 70 kDa protein 2 (HSPA2) (Sigma) or sperm acrosome associated 3 (SPACA 3) (Abcam, Cambridge, UK) diluted at 1:100 for 1 h at 37°C in 5% CO_2. The samples were then centrifuged twice at 500g for 5 min and incubated with Alexa Fluro 488 conjugated goat anti-rabbit IgG for one hour at 37°C in 5% CO_2. (1:1000; Invitrogen, MA, USA). The samples were centrifuged twice at 500g for 5 min and resuspended into EBSS/ no BSA for flow consistency (Beckman Coulter, CA, USA). Data were analyzed using FlowJo v10.0.7 software (Copyright Tree Star, Inc. Stanford Jr. University).

ZP-bound and unbound spermatozoa were allowed to air-dry in a small area on a sterile glass slide at 37°C. The slides were gently rinsed with distilled water thrice. The samples were individually incubated with primary antibodies against HSPA2 (Sigma) or SPACA3 (Abcam) diluted at 1:100 overnight at 4°C. The slides were gently rinsed with distilled water twice. The samples were then incubated with Alexa Fluro 555 conjugated goat anti-rabbit IgG for one hour at 37°C in 5% CO_2. (1:1000; Invitrogen), rinsed gently with distilled water twice and immediately mounted with fluorescent mounting medium (Dako). The stained spermatozoa were observed under a fluorescence microscope (Nikon Eclipse Ti, Tokyo, Japan) at a magnification of 600x or a Carl Zeiss LSM 880 with Ariyscan 2 at a magnification of 630x (Carl Zeiss, NY, USA) using excitation/emission wavelengths of 555 nm/580 nm. A minimum of 100 spermatozoa/sample with positive signals across their head regions was quantified to determine the expression patterns. The fluorescence intensities were evaluated using Image J analysis software (Version 1.48 v; NIH, USA)

2.8 Evaluation of sperm morphology

ZP-bound and unbound spermatozoa were smeared on a glass slide and allowed to air-dry at 37°C. The slides were then gently

rinsed with distilled water once. The samples were fixed with the fixative solution (methanol-based solution) for 15 s and stained with the staining solution 1 (buffered solution of Eosin Y) for 10 s followed by the staining solution 2 (buffered solution of thiazine dyes) for 10 s. The excess solution was allowed to drip off the slides between steps. The samples were gently rinsed with distilled water once and allowed to air-dry. Spermatozoa were assessed manually under oil immersion using a light microscope (Zeiss, Gottingen, Germany) at a magnification of 1000x. A minimum of 100 spermatozoa/sample was quantified according to the WHO strict criteria (27) to determine the percentage of normal morphology.

2.9 Evaluation of DNA fragmentation rates by terminal deoxynucleotidyl transferase dUTP nick end labelling

ZP-bound and unbound spermatozoa were allowed to air-dry in a small area on a sterile glass slide at 37°C. The slides were then gently rinsed with distilled water thrice. The washed spermatozoa were fixed with 2% paraformaldehyde for 1 h at room temperature and gently rinsed with PBS twice. After fixation, the spermatozoa were permeabilized with freshly prepared 0.1% Triton X-100 in sodium citrate for 2 min at 4°C and rinsed with PBS twice. The permeabilized spermatozoa were incubated in 50 µL of reaction mixture containing terminal deoxynucleotidyl transferase (TdT) and fluorescein- dUTP (*In Situ* cell death detection kit, fluorescein, Sigma-Aldrich, MA, USA) in a 1:9 ratio for 1 hour at 37°C in the dark. The slide was then rinsed with PBS twice and mounted with fluorescent mounting medium (Dako). The TUNEL-positive spermatozoa were observed under a fluorescence microscope (Nikon Eclipse Ti, Tokyo, Japan) at a magnification of 600x using excitation/emission wavelengths of 488nm/530nm. A minimum of 100 spermatozoa/sample was quantified to determine the percentage of DNA fragmentation rates [(number of TUNEL-positive spermatozoa with bright, green fluorescence over the head regions/total number of spermatozoa) x 100%].

2.10 Evaluation of DNA damages by comet assay

ZP-bound and unbound spermatozoa were mixed with the molten low-melting point agarose (Trevigen, MD, USA) at 1:5 ratio (V/V) on a Comet slide (Trevigen). The mixture was allowed to solidify at 4°C in the dark for 10 min. The slides were then immersed in cold lysis buffer (Trevigen) at 4°C for 30 min. After removing the excess buffer, the slides were incubated in freshly prepared alkaline solution (pH~13) for 30 min. The slides were then transferred into a horizontal electrophoresis tank containing freshly prepared alkaline buffer for electrophoresis at 21V for 30 min. The slides were washed in distilled water twice for 10 min followed by 70% ethanol for 5 min. The samples were allowed to air-dry at 37°C. The dried samples were then incubated with SYBR Green I (Molecular Probes, OR, USA) at room temperature in the dark for 5 min. After removing the excess staining solution, the COMET-positive spermatozoa were observed under a fluorescence microscope (Nikon Eclipse Ti, Tokyo, Japan) at a magnification of 600x using excitation/emission wavelengths of 488nm/530nm. The extent of DNA damage in a minimum of 100 spermatozoa/sample was determined by measuring the percentage of tail DNA ((tail intensity/total intensity) x 100%) and the tail moment (%DNA in the comet tail x tail length) using the COMET assay II software (Perceptive Instruments, Haverhill, UK).

2.11 Evaluation of chromatin integrity by acridine orange staining

Air-dried and washed ZP-bound and unbound spermatozoa in a small area on a sterile glass slide as described above were fixed with Carnoy's solution (acetic acid-methanol in a 3:1 ratio) overnight at 4°C. The slides were gently rinsed with PBS twice and allowed to air-dry prior to the staining procedure. The AO staining solution was prepared daily by adding 1% AO stock solution (Thermofisher, MA, USA) to a mixture of 0.1M citric acid and 0.3M Na_2HPO_4, pH 2.5. The spermatozoa were incubated with the staining solution for 5 min at 37°C in the dark and gently rinsed with distilled water twice. The stained spermatozoa were immediately observed under a fluorescence microscope (Nikon Eclipse Ti, Tokyo, Japan) at a magnification of 600x using excitation/emission wavelengths of 488nm/530nm. The percentage of spermatozoa with normal/abnormal chromatin structure was determined by scoring a minimum of 100 spermatozoa/sample with bright, green fluorescence (double-stranded DNA) and those with orange/yellow fluorescence (single-stranded DNA).

2.12 Evaluation of protamine deficiency by chromomycin A3 staining

Air-dried and washed ZP-bound and unbound spermatozoa were fixed with Carnoy's solution (acetic acid-methanol in a 3:1 ratio) at 37°C for 10 min. The fixed spermatozoa were incubated with 0.25mg/ml CMA_3 (Sigma) in Mcllvaine buffer 0.1M citric acid and Na_2HPO_4•$7H_2O$, pH 7.0, containing 10 mM $MgCl_2$ for 20 min at room temperature. The slides were gently rinsed with PBS and mounted with fluorescent mounting medium (Dako). The stained spermatozoa were observed under a fluorescence microscope (Nikon Eclipse Ti, Tokyo, Japan) at a magnification of 600x using excitation/emission wavelengths of 488nm/580nm. The degree of protamine deficiency was determined by quantifying the overall signal intensity of a minimum of 100 spermatozoa with yellow fluorescence (CMA3-positive).

2.13 Evaluation of methylation level by immunostaining

Air-dried and washed ZP-bound and unbound spermatozoa were fixed with Carnoy's solution (acetic acid- methanol in a 3:1

ratio) at 4°C for 20 min and gently rinsed with PBS with 0.5% Tween twice. For sperm decondensation, the fixed spermatozoa were incubated with 1M Tris-HCl, pH 9.5, containing 25 mM dithiothreitol (DTT) for 20 min at room temperature and gently rinsed with PBS twice. The decondensed spermatozoa are denatured by incubation with 6N HCl for 15 min and gently rinsed with PBS twice. The denatured spermatozoa were stained with anti-5-methylcytosine (5-mC) (Abcam) overnight at 4°C and gently rinsed with PBS twice. The samples were then incubated with Alexa Fluro 488 conjugated goat anti-mouse IgG for one hour at 37°C (1:1000; Invitrogen), rinsed gently with distilled water twice and immediately mounted with fluorescent mounting medium (Dako). The stained spermatozoa were observed under a fluorescence microscope (Nikon Eclipse Ti, Tokyo, Japan) at a magnification of 600x using excitation/emission wavelengths of 488 nm/525 nm. The level of methylation in spermatozoa was determined by quantifying the overall signal intensity of a minimum of 100 spermatozoa with green fluorescence (5-Mc-positive).

2.14 Data analysis

All experimental data were expressed as mean ± standard deviation (Mean ± SD) or median (range). Statistical software (GraphPad Prism 9.1.0, GraphPad software, CA, USA) was used to analyze the data. Two tailed unpaired t-test was used to examine the differences between the ZP-bound and unbound sperm subpopulations. If the data failed the normality test, Mann-Whitney (non-parametric) test was used to perform statistical analysis. A probability value of < 0.05 was considered as statistically significant.

3 Results

3.1 Retrieval of ZP-bound human spermatozoa by continuous spermatozoa-ZP coincubations

The total number of spermatozoa tightly bound to the ZP per assay was quantified at 2 h intervals during the 6 h continuous coincubation (Figure 1A). An average of 150 ZP-bound spermatozoa was retrieved per assay within the first 2 h of coincubation. The time-course study showed that the total number of ZP-bound spermatozoa gradually decreased over time and eventually plateaued at 20 h (Figure 1A). Approximately 0.03% of the motile spermatozoa in the incubation droplet containing $1x10^6$ spermatozoa/mL bound to the ZP within the first 6-h incubation period. Incubation of spermatozoa for up to 6-h had no adverse effects on sperm viability, motility and DNA integrity (Figures 1B-D). The number of ZP-bound spermatozoa in two continuous assays with or without the replacement of oocyte at 4-h was comparable (Figure 1E), suggesting that reusing the same group of oocytes throughout the entire incubation period did not impair the binding interaction.

3.2 Immunodetection of acrosome reaction and protein markers on ZP-bound spermatozoa

The acrosome reaction rates of ZP-bound spermatozoa recovered at 15 and 30 min (15.7% ± 4.2 and 14.5% ± 2.7) (Figure 2) were comparable to the spontaneous acrosome reaction rates of those in the control without prior exposure to the ZP. The ZP-bound spermatozoa recovered at 60 and 120 min (63.7% ± 10.1 and 70.9% ± 4.4 vs. 26.3% ± 11.7, $p<0.05$) (Figure 2) had higher acrosome reaction rates than the unbound ones.

The expression of HSPA2 and SPACA3 on capacitated human spermatozoa were individually evaluated by flow cytometry. The protein markers were positively present (HSPA2: 36.3 ± 6.5% and SPACA3: 17.9 ± 0.5%) (Supplementary Figure 1) on the capacitated human spermatozoa. Confocal microscopy revealed markedly granular pattern of staining for these molecules on capacitated spermatozoa (Figures 3A, B). HSPA2 and SPACA3 localized to the head regions of capacitated human spermatozoa (Figures 3C, D). To examine their expression solely on the plasma membrane, the optimal time-point to recover acrosome-intact, ZP-bound spermatozoa was 30 min. Approximately 86% of the ZP-bound spermatozoa recovered at 30 min were HSPA2- or SPACA3-positive (Figures 3E, F). ZP-bound spermatozoa recovered at 30 min had a higher percentage of positive HSPA2 (85.8% vs. 45.9%, $p<0.05$) and SPACA3 signals (86.3% vs. 30.5%, $p<0.05$) than the unbound ones (Figure 3). The signal intensities of both markers were stronger in the ZP-bound spermatozoa recovered at 30 min than the unbound ones ($p<0.05$) (Figures 3G, H).

3.3 Morphology evaluation of ZP-bound and unbound spermatozoa

The number of morphologically normal spermatozoa was significantly higher in the ZP-bound spermatozoa recovered at 30 min than in the unbound ones (Figure 4), indicating a relationship between the morphology and ZP-binding ability of spermatozoa.

3.4 Evaluation of genetic quality of ZP-bound and unbound spermatozoa

Comet and TUNEL assays (Supplementary Figures 2A, B) were used to evaluate DNA fragmentation rates of ZP-bound and unbound spermatozoa. In the comet assay, the ZP-bound spermatozoa had a significantly lower level of tail DNA (27.6% vs. 40.2%, $p<0.05$) (Figure 5A) and tail moment (15.4% vs 22.1%, $p<0.05$) (Figure 5A) than the unbound ones. Consistently, the number of TUNEL-positive spermatozoa was significantly lower in the ZP-bound than in the unbound sperm subpopulations (4.1% vs. 15.5%, $p<0.05$) (Figure 5B), correlating the ZP-binding ability and DNA integrity of spermatozoa. A high proportion of ZP-bound spermatozoa with intact DNA was found in all sample groups, even

10.3389/fendo.2023.1135973

A

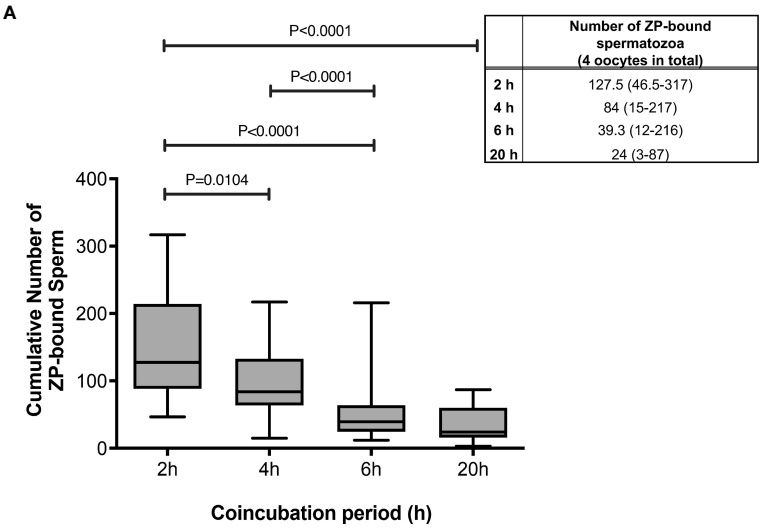

	Number of ZP-bound spermatozoa (4 oocytes in total)
2 h	127.5 (46.5-317)
4 h	84 (15-217)
6 h	39.3 (12-216)
20 h	24 (3-87)

B

Time	0 h	2 h	4 h	6 h
Total Number of sperm	253.0± 66.4	263.8± 39.6	248.4± 30.9	255.8± 34.8
Motility %	93.6± 5.6	91.2± 7.8	94.0± 5.6	94.8± 5.8
Progressive motility %	85.2± 6.8	82.6± 8.4	82.0± 9.8	84.2± 3.3
Non-progressive motiltiy %	10.2± 4.3	10.0± 3.0	13.2± 9.6	12.8± 3.1
immotility %	4.8± 4.7	7.4± 7.3	4.8± 2.9	3.0± 2.0
Average path velocity (VAP) μm/s	25.1± 1.7	25.2± 1.5	26.3± 3.0	25.6± 1.5
Straight line velocity (VSL) μm/s	10.8± 1.8	10.6± 0.4	10.8± 1.8	11.0± 2.6
Curvilinear velocity (VCL) μm/s	92.8± 13.2	95.6± 5.1	101.6± 8.8	100.7± 7.9
Lateral Amplitude μm	3.5± 0.7	3.7± 1.1	4.1± 2.1	3.8± 0.9
Beat Frequency Hz	54.1± 1.8	53.1± 1.4	54.7± 2.3	54.9± 1.4
Straightness %	43.6± 7.8	41.0± 2.5	40.0± 3.2	42.2± 6.1
Linearity %	15.8± 4.2	15.0± 2.5	15.4± 4.5	16.0± 6.5
Elongation of sperm head %	65.8± 2.4	63.4± 3.2	63.4± 1.8	64.6± 3.7
Area μm	5.9± 0.8	5.7± 0.5	5.7± 1.0	5.2± 0.8

C D E

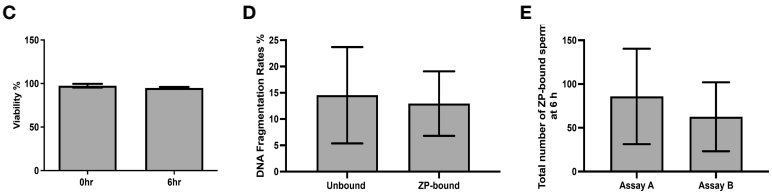

FIGURE 1
The total number of ZP-bound spermatozoa over the 6-h and 20-h incubation. **(A)** The number of spermatozoa tightly bound to the oocytes was counted at 2 h intervals during the 6-h incubation. There was a large variation in the number of ZP-bound spermatozoa, but the decreasing trend persisted in all samples. All data are represented as median (range) (n=24 for 6-h; n=6 for 20-h, p<0.05). **(B)** Effects of prolonged incubation on sperm motility at intervals of 0, 2, 4, 6 h. **(C, D)** Effects of prolonged incubation on sperm viability and DNA integrity at 0 and 6 hr. **(E)** The total number of ZP-bound spermatozoa with (Assay A) /without (Assay B) the replacement of fresh oocytes at 4 hr. All data are represented as mean ± SD (n=5).

in raw semen with a high DNA fragmentation rate of 19.1% (Supplementary Figure 3). AO staining (Supplementary Figure 2C) was used to evaluate the chromatin structure and to differentiate spermatozoa with normal double-stranded DNA from those with abnormal single-stranded DNA. The number of spermatozoa with green fluorescence was significantly higher in the ZP-bound than the unbound spermatozoa (93.1% vs. 64.3%, p<0.05) (Figure 5C). There was a small proportion of ZP-bound spermatozoa with red fluorescence (6.4% on average) in both swim-up and raw sample groups (Supplementary Figure 3), indicating a correlation between the ZP-binding ability and chromatin integrity of spermatozoa.

3.5 Evaluation of protamination and methylation of ZP-bound and unbound spermatozoa

CMA3 staining (Supplementary Figure 2D)was used to indirectly evaluate the degree of protamination in spermatozoa. CMA3 is a fluorochrome that specifically binds to the same location as protamines at the GC-rich sequences. Spermatozoa with protamine deficiency appeared bright yellow whilst those with proper protamination fluoresced light yellow with different degrees of signal intensity (Figure 5D). The level of CMA3 positivity was significantly lower in ZP-bound than in the

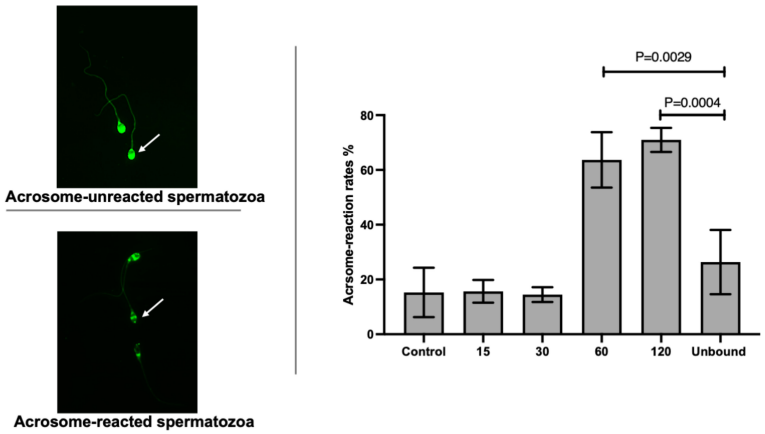

FIGURE 2
Time-course study of acrosome-reaction rates in ZP-bound spermatozoa. Acrosomal status of the control, unbound spermatozoa, ZP-bound spermatozoa (recovered at 15, 30, 60 and 120min) was determined by FITC-PSA. All data are represented as mean ± SD (n=4, p<0.05).

unbound spermatozoa (p<0.05) (Figure 5D), suggesting that the human ZP selectively bound to spermatozoa with high degree of protamination. Immunofluorescent staining for the methylated regions (Supplementary figure 2E) was used to evaluate the overall methylation level of ZP-bound and unbound spermatozoa. Spermatozoa displayed varying degrees of green fluorescence depending on the DNA methylation level (Figure 5E). The overall methylation level was higher in ZP-bound than in the unbound spermatozoa (Figure 5E), as reflected by the signal intensity.

4 Discussion

Spermatozoa-ZP binding assay was first established by Overstreet and Hembree to examine the interaction between the non-viable oocytes and spermatozoa *in vitro* (29). Considering the small number of motile spermatozoa with ZP-binding ability in fertile donors (25, 30), it is logical to assume that this species-specific interaction might shed light on the potential use of ZP to select high-quality spermatozoa *in vitro*. In this study, the ZP-bound spermatozoa were found with higher rates of normal morphology, acrosome reaction rates, and DNA integrity when compared with the controls, consistent with previous studies demonstrating the selective nature of ZP to spermatozoa to fertilization-competent spermatozoa (31–33). Clinical studies using ZP-selected spermatozoa demonstrated minimal advantages on the fertilization and implantation rates but greatly improved the embryo qualities and pregnancy rates (34–37).

In this study, a modified continuous coincubation assay was used to collect spermatozoa without ZP-binding ability by gradually removing the ZP-bound spermatozoa from the incubation droplet at 2-h intervals over a 6-h period. Our results demonstrated that the total number of ZP-bound spermatozoa varied distinctively among samples, consistent with previous findings reporting on the differences in the number of motile spermatozoa with ZP-binding ability between fertile and infertile men (25). The time-course data indicated that about 50% of the motile spermatozoa with ZP-binding ability bound to the ZP within the first 2 h and gradually decreased over time until the end of coincubation at 6 hr. In comparison with a previous study (25), the overall percentage of ZP-bound spermatozoa recovered by our protocol was significantly lower (0.03% vs. 14.0% in fertile men). The discrepancy is likely due to the difference in protein concentration of BSA or other specific molecules related to ZP-binding ability. The number of ZP-bound spermatozoa is higher in culture medium supplemented with human serum than with BSA (38). Liu et al. also reported that the number of ZP-bound spermatozoa exponentially increased over 6 h, which differed from our results. Capacitation is a time-dependent process (39). It is possible that the components of the culture medium could affect capacitation during which the spermatozoa acquire ZP-binding ability (40), although human spermatozoa tend to complete capacitation within 3 h (41, 42). We also performed additional tests to confirm that the repeated uses of oocytes did not affect the ZP-binding results and that the extended incubation had no negative impact on the sperm parameters, excluding the possibility that the low ZP-binding efficiency was caused by progressive loss of functional and/or structural properties of the ZP and spermatozoa during incubation.

Spermatozoa-ZP binding interaction involves the recognition of ligands by the protein receptors on the plasma membrane of capacitated spermatozoa. Ultrasensitive analysis by mass spectrometry revealed that human ZP glycans are terminated with a high abundance of Siayl-LewisX (SLeX) sequences (43). Treatment targeting against SLeX sequences inhibits approximately 70% of spermatozoa-ZP binding (43). Moreover, recombinant human ZP-proteins with glycosylation different from their native counterparts are capable of binding to human spermatozoa (44, 45). The results suggested that both glycan-protein and protein-protein interactions are involved in spermatozoa-ZP binding. Proteomic studies identified a list of potential ZP receptors located on the plasma membrane of capacitated spermatozoa (46–48). During capacitation, dynamic changes occur on the sperm proteome to facilitate conformational modifications or exposure of ZP receptors located on the plasma

10.3389/fendo.2023.1135973

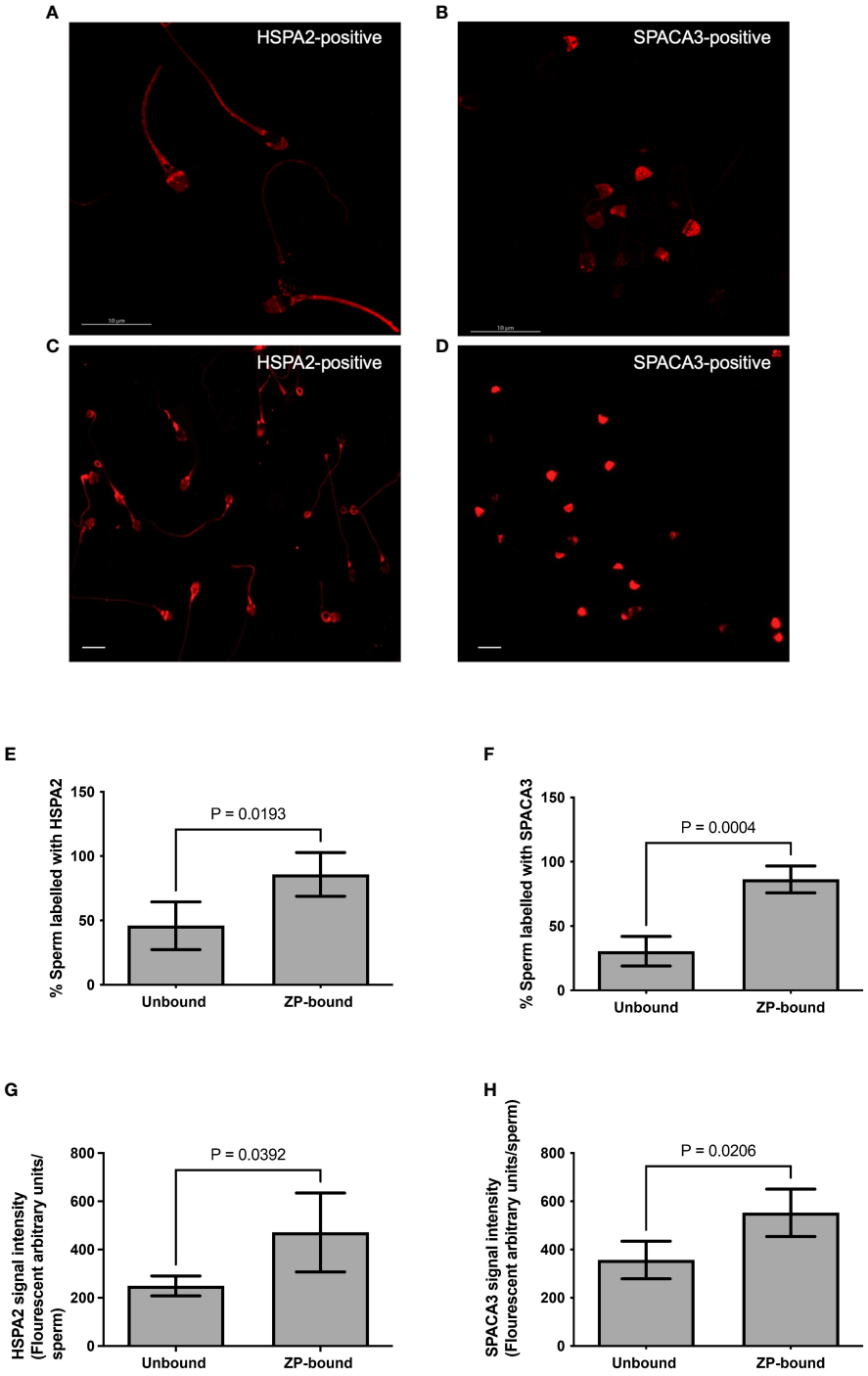

FIGURE 3
Immunolocalization of HSPA2 and SPACA3 on capacitated human spermatozoa. **(A, B)** Capacitated spermatozoa were labelled with anti-HSPA2 and SPACA3 antibodies (diluted 1:100) respectively followed by Alexa-555 secondary antibodies. The images captured using confocal microscopy showed granular staining patterns of HSPA2 and SPACA3 on spermatozoa. Scale bar = 10 μM. **(C)** HSPA2 was localized to the peri-acrosomal region, equatorial segment, post-acrosomal region, mid-piece and the sperm tail. **(D)** SPACA3 was localized to the acrosomal region. Scale bar=200 uM. **(E, F)** Quantification of ZP-bound recovered at 30 min and unbound spermatozoa showing positive staining with HSPA2 and SPACA3 at the head regions. All data are represented as mean ± SD (n=4, $p<0.05$). **(G, H)** Fluorescence intensity analysis of each protein marker was performed by the Image J software. All data are represented as mean ± SD (n=4, $p<0.05$).

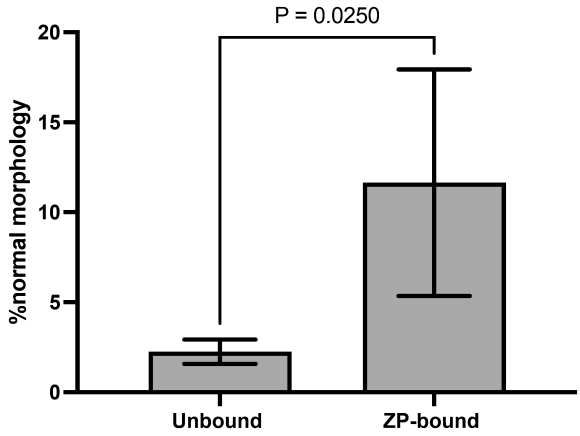

FIGURE 4
Morphology evaluation of ZP-bound and unbound spermatozoa. ZP-bound and unbound spermatozoa were classified as having normal or abnormal morphology according to the WHO strict criteria. All data are represented as mean ± SD (n=5, $p<0.05$).

membrane of acrosome-intact spermatozoa (49, 50). Soon after ZP-binding, acrosome reaction is initiated in ZP-bound spermatozoa to facilitate the subsequent penetration through the ZP. Thus, the acrosomal status is an indirect evaluation of sperm fertilization potential. Many membrane proteins, such as sperm adhesion molecule 1 (also known as PH-20), are also found on the inner acrosomal region of spermatozoa, which become exposed after the ZP binding interaction (51). In this study, we determined the optimal time-point to collect acrosome-intact, ZP-bound spermatozoa. Acrosome reaction is a time-dependent process. Consistently, after binding to the ZP, mouse spermatozoa remain acrosome-unreacted for approximately 40 min before commencing acrosome-reaction (52). Using the time-lapse fluorescence microscopy, it has been demonstrated that calcium ionophore (A23187) and progesterone induce acrosome reaction in human spermatozoa within 12 min (53). There is a lack of time-lapse study on the acrosome reaction rates of ZP-bound spermatozoa in humans. Our results demonstrated that majority of spermatozoa bound to the ZP for less than 30 min were acrosome-intact and approximately 60% of the ZP-bound spermatozoa became acrosome-reacted after 60 min. The ZP-bound spermatozoa recovered at 60 and 120 min had significantly higher acrosome reaction rates than the unbound ones.

In this study, the ZP-bound spermatozoa were recovered within 30 min to maximize the possibility of collecting acrosome-intact spermatozoa. The expression levels of HSPA2 and SPACA3 were about two times higher on the ZP-bound spermatozoa than on the unbound ones. HSPA2 is a testis-enriched member of the 70 kDa heat shock proteins (HSP-70) family, which promotes proper protein folding, translocation of intracellular proteins, and assembly of multimeric protein complexes (54). In humans, the HSPA2 gene expression is downregulated in men with azoospermia (55), varicocele and oligozoospermia (56), and idiopathic oligoteratozoospermia (57). The expression level of HSPA2 is positively correlated with maturity (58, 59), ability of binding to ZP and cumulus complexes (58, 60), and fertilization potential (58, 61–63) of human spermatozoa. Emerging studies suggest that HSPA2 remains predominantly intracellular in human spermatozoa, which serves as a chaperone to mediate the assembly of multimeric protein complexes located on the anterior region of the sperm head for ZP binding (64–66). During capacitation, HSPA2 is translocated from the inner to the outer leaflet of the plasma membrane, leading to an increased level of HSPA2 on spermatozoa (62, 67). HSPA2 interacts with the sperm adhesion molecule 1 (SPAM1) and arylsulfatase A (ARSA) to form an acrosomal domain for spermatozoa-ZP recognition. A lack of HSPA2 is found in infertile patients with defective ZP-binding ability (64). In this study, our results suggested that the expression level of HSPA2 on spermatozoa was reflective of their ZP-binding ability.

SPACA3, also known as SLLP1, is highly homologous with c-lysozyme and retains the putative substrate-binding residues conserved across mammals, such as humans and mice, for the binding to oligosaccharides of N-acetylglucosamine (GlcNAc) (68, 69). In mice, SLLP1 specifically binds to the receptors within the perivitelline space and on the plasma membrane of oocyte *in vitro* (70). The recombinant SLLP1 and antibodies directed against SLLP1 suppress the binding of spermatozoa to cumulus intact and ZP-free oocytes (70). This observation implies a functional role of SLLP1 in spermatozoa-oolemma interaction during fertilization. It is logical to assume that SLLP1 can participate in the spermatozoa-ZP binding interaction since GlcNAc has been identified on mammalian ZP (71–73). Partial inhibition of spermatozoa-ZP binding occurs when capacitated spermatozoa are pre-treated with GlcNAc or ZP is pre-incubated with glycosidase N-acetylglucosaminidase *in vitro* prior to hemizona assay (74, 75). The involvement of SLLP1 in spermatozoa-ZP interaction was further supported by a modified spermatozoa-ZP binding assay in which the calcium ions in the culture and co-incubation medium were replaced by the strontium ions to ensure that the spermatozoa were allowed to undergo capacitation required for ZP- binding, but not acrosome reaction following the binding interaction (76). This experimental condition demonstrated the inhibitory effects of exogenous GlcNAc specifically on

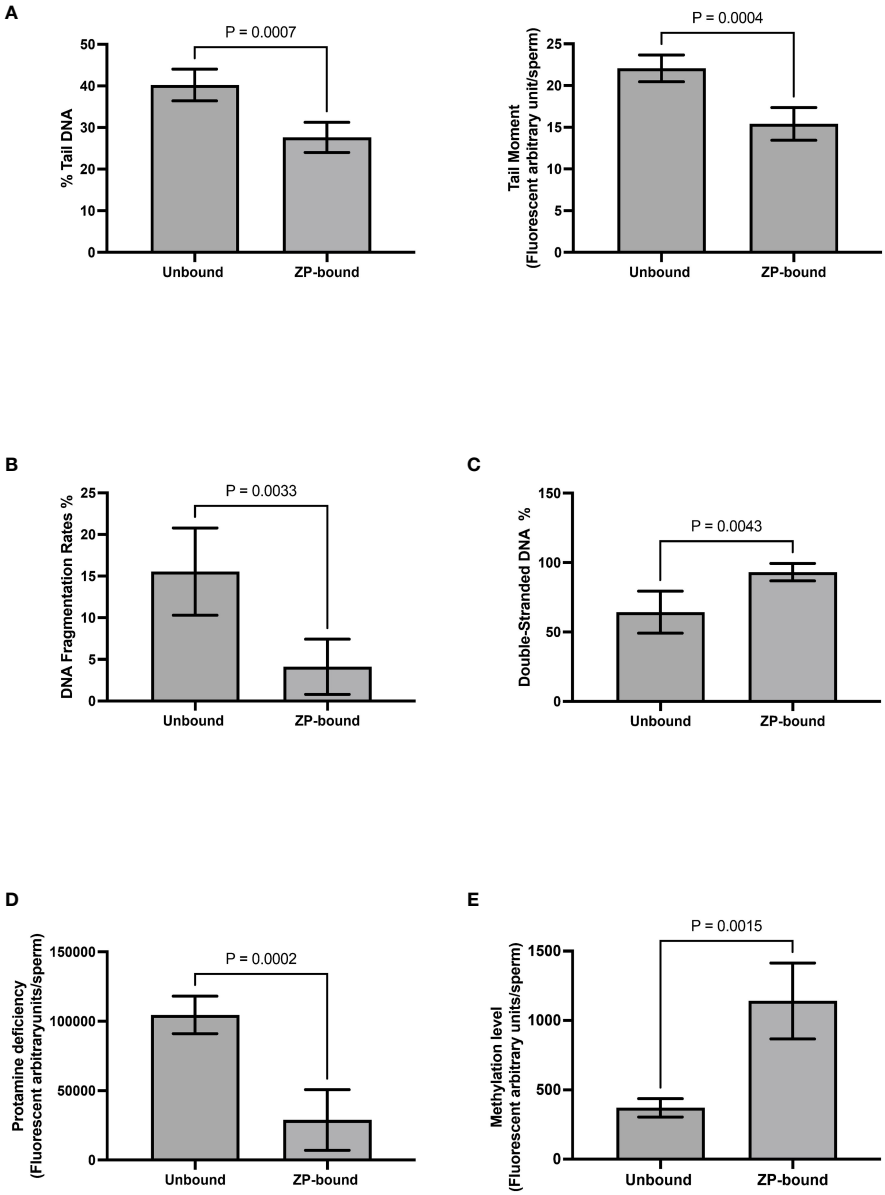

FIGURE 5
Evaluation of genetic qualities and epigenetic profile of ZP-bound and unbound spermatozoa. Quantification of **(A)** Comet-positive spermatozoa with different levels of DNA damages as reflected by the (Left) %tail DNA and (Right) tail moment **(B)** TUNEL-positive spermatozoa **(C)** AO-stained spermatozoa with double-stranded DNA in green fluorescence **D)** CMA3-positive spermatozoa with different levels of protamine deficiency as reflected by the yellow fluorescence intensity. **(E)** 5-Mc-positive spermatozoa with different levels of methylation as reflected by the green fluorescence intensity. All data are represented as mean ± SD (n=5 for **(A–E)**, $p<0.05$).

spermatozoa- ZP binding (76). According to our results, neither HSPA2 nor SPACA3 were uniformly expressed on the entire population of ZP-bound spermatozoa, corroborating previous findings that the absence of a single protein receptor is highly unlikely to cause complete failure of spermatozoa-ZP binding because the ZP-receptor is a multimolecular structure assembled during capacitation (23, 77). Nevertheless, the expression level of a single marker could reflect the ability of spermatozoa acquiring the appropriate molecules required for ZP-binding during transit through the reproductive tract. The fluorescence intensity of protein markers can serve as an additional surrogate marker relevant to sperm fertilizing capability and genetic quality, which might in turn increase the discriminating power of the conventional semen analysis. If the protein markers are to become useful as diagnostic tools, clinical samples with varying degrees of ZP-binding ability should be collected to establish clinical thresholds of protein expressions.

DNA damages in spermatozoa are primarily induced by abortive apoptosis during spermatogenesis, chromatin remodeling during spermiogenesis, and oxidative stress during migration through the male reproductive tract (78). Under physiological circumstances, a low level of reactive oxygen species (ROS) is needed for physiological functions such as cellular activities and signaling pathways in spermatozoa (79). Oxidative stress as a result

of excessive ROS production is closely related to male infertility (80). In some cases, spermatozoa with genetic abnormalities can retain their fertilizing ability leading to fertilization success, but the genetic defects might later manifest themselves as late paternal effects (81), resulting in a higher rate of suboptimal embryo development, pregnancy failure and pregnancy complications (82, 83). The level of DNA fragmentation is associated with lower pregnancy rates in IVF cycles following conventional insemination but not in intracytoplasmic sperm injection cycles (84), although increased miscarriage rates (84) and reduced live birth rates (85) are observed in both conventional insemination and intracytoplasmic sperm injection cycles. The ZP-binding ability of spermatozoa was closely related to their DNA integrity and chromatin status. Both alkaline Comet and TUNEL assays are developed to examine the overall level of DNA damages in spermatozoa. Alkaline Comet assay is a relatively sensitive method for measurement of single and double-strand breaks in spermatozoa. In this method, the fragmented DNA migrate out of the sperm head towards the anode forming a comet tail under an applied electrical field. The degree of DNA fragmentation is reflected by the fluorescence intensity and the length of the Comet tail. A high degree of DNA fragmentation measured by the comet assay is correlated with the lower rates of fertilization, good embryo development and implantation (86). TUNEL assay involves the attachment of fluorescently modified nucleotide to the free 3'- OH terminal of single- and double-stranded DNA mediated by TdT (87). The DNA fragmentation index is negatively correlated with inferior sperm parameters in terms of concentration, viability, motility, and morphology (88, 89). In this study, both methods demonstrated that the number of spermatozoa with fragmented DNA was significantly lower in ZP-bound spermatozoa than the unbound ones, implicating the relationship between the ZP-binding ability and genetic quality of spermatozoa.

AO intercalates into normal double-stranded DNA as a monomer and fluoresces green as opposed to binding to the denatured, single-stranded DNA as an aggregate which fluoresces yellow to red depending on the extent of the damages (90). The number of spermatozoa with green fluorescence was significantly higher in the ZP-bound spermatozoa than in the unbound ones, suggesting that the spermatozoa-ZP interaction is highly selective for spermatozoa with normal, double-stranded DNA. In contrast to the TUNEL results, the AO staining results demonstrated that the swim-up method failed to eliminate spermatozoa with abnormal genetic integrity; the number of spermatozoa with yellow-red fluorescence in post-swim-up samples was comparable to those in raw samples, consistent with previous findings that showed the lack of correlation between motility and chromatin integrity of spermatozoa (91).

In addition to genetic integrity, the epigenetic patterns of spermatozoa have been linked to embryonic development, implantation success, and the offspring health following ICSI (92, 93). Spermatozoa undergo epigenetic modifications including chromatin remodeling, DNA methylation, and non-coding RNAs to regulate transcriptional activities and gene expression at post-transcriptional level (94, 95). Aberrant epigenetic profiles in spermatozoa have been implicated in male idiopathic infertility. Protamine protein 1 and 2 (P1 and 2) are equally distributed in spermatozoa of healthy men. P1/2 imbalance is associated with poor sperm parameters and male infertility (96–99). Furthermore, abnormal methylation patterns at specific loci, such as H-19 and mesoderm-specific transcript (MEST), have been found in men with male-factor infertility (100–103). Aberrant global methylation levels are associated with suboptimal sperm parameters (104–106) and male infertility (107, 108). Our results indicated that the ZP-binding ability of spermatozoa was closely related to their epigenetic patterns in terms of protamination degree and global methylation level. The examination of methylation status at specific loci might definitively answer the question as to whether hypomethylation or hypermethylation is the major factor leading to suboptimal ZP-binding ability. To pinpoint the specific locus associated with ZP-binding ability, future investigation is needed to examine the DNA methylation profile of ZP-bound spermatozoa by single-cell bisulfite sequencing (109, 110). While the complicated staining and quantification procedures restrict wide application of genetic evaluation in clinical settings, future investigation should seek to develop a highly robust, indirect evaluation of sperm quality metrics by image analysis of sperm morphology associated with genetic integrity (111) and epigenetic pattern to establish a comprehensive profile of clinical samples.

5 Conclusion

Although conventional semen analysis is useful for establishing a fertility profile of men, it fails to provide diagnostic information regarding the sperm fertilization potential. The spermatozoa-ZP interaction serves as an integral part of the natural sperm selection mechanisms *in vivo*, which can potentially be used for sperm evaluation and selection in clinical settings. An early detection of defective ZP-binding ability in men with normal semen parameters could be offered intracytoplasmic sperm injection instead of conventional insemination, preventing them from financial and psychological sufferings caused by the low or no fertilization rates following conventional insemination. HPSPA2 and SPACA3 are the protein markers associated with the ZP-binding ability of spermatozoa. There was a quantitative difference in the expression level of HSPA2 and SPACA3 between acrosome intact, ZP-bound and unbound spermatozoa. Although the ZP-receptor is likely a multi-molecular structure, the expression level of a single marker could reflect the ability of spermatozoa acquiring the appropriate molecules required for ZP-binding during transit through the reproductive tract. Our results demonstrated that the ZP-binding ability of spermatozoa was closely related to their genetic quality in terms of DNA integrity, chromatin structure, protamination degree and global methylation level. Human ZP was highly selective for genetically normal spermatozoa with distinct epigenetic profiles. If the spermatozoa-ZP interaction is to become useful as a clinical tool, clinical samples with varying degrees of ZP-binding ability should be collected to establish a representative database for identification of high-quality spermatozoa by image analysis of sperm morphology. Taken together, the development of a robust and reproducible selection method incorporating the ZP-

binding ability of spermatozoa might improve the overall workflow and the pregnancy outcomes in ART.

Data availability statement

The original contributions presented in the study are included in the article/Supplementary Material. Further inquiries can be directed to the corresponding authors.

Ethics statement

The studies involving human participants were reviewed and approved by Institutional Review Board of the University of Hong Kong/Hospital Authority Hong Kong West Cluster. The patients/participants provided their written informed consent to participate in this study.

Author contributions

WY and PC conceived and designed the project. EL, BL, and KL collected samples and conducted experiments. EL and BL analyzed and interpreted the collected data. EL and PC wrote the first draft of the manuscript. C-LL, XT, KL, RL, EN, WY, and J-PO revised the manuscript. All authors contributed to the article and approved the submitted version.

Funding

This work was supported in part by the Health and Medical Research Fund, the Food and Health Bureau, The Government of the HKSAR (07182446), the High Level-Hospital Program, Health Commission of Guangdong Province, China (HKUSZH201902015), and HKU-SZH Fund for Shenzhen Key Medical Discipline (SZXK2020089).

Acknowledgments

We appreciated all participants of this study and the assistance from the andrology laboratory at Family Planning Association of Hong Kong and the IVF laboratory at Queen Mary Hospital, Hong Kong.

Conflict of interest

The authors declare that the research was conducted in the absence of any commercial or financial relationships that could be construed as a potential conflict of interest.

Publisher's note

Supplementary material

The Supplementary Material for this article can be found online at: https://www.frontiersin.org/articles/10.3389/fendo.2023.1135973/full#supplementary-material

References

1. Agarwal A, Mulgund A, Hamada A, Chyatte MR. A unique view on male infertility around the globe. *Reprod Biol Endocrinol* (2015) 13:37. doi: 10.1186/s12958-015-0032-1

2. Kushnir VA, Barad DH, Albertini DF, Darmon SK, Gleicher N. Systematic review of worldwide trends in assisted reproductive technology 2004-2013. *Reprod Biol Endocrinol* (2017) 15(1):6. doi: 10.1186/s12958-016-0225-2

3. Simon L, Proutski I, Stevenson M, Jennings D, McManus J, Lutton D, et al. Sperm DNA damage has a negative association with live-birth rates after IVF. *Reprod BioMed Online* (2013) 26(1):68–78. doi: 10.1016/j.rbmo.2012.09.019

4. Chapuis A, Gala A, Ferrières-Hoa A, Mullet T, Bringer-Deutsch S, Vintejoux E, et al. Sperm quality and paternal age: effect on blastocyst formation and pregnancy rates. *Bas Clin Androl* (2017) 27:2. doi: 10.1186/s12610-016-0045-4

5. Leung ETY, Lee CL, Tian X, Lam KKW, Li RHW, Ng EHY, et al. Simulating nature in sperm selection for assisted reproduction. *Nat Rev Urol* (2022) 19(1):16–36. doi: 10.1038/s41585-021-00530-9

6. Stevanato J, Bertolla RP, Barradas V, Spaine DM, Cedenho AP, Ortiz V. Semen processing by density gradient centrifugation does not improve sperm apoptotic deoxyribonucleic acid fragmentation rates. *Fertil Steril* (2008) 90(3):889–90. doi: 10.1016/j.fertnstert.2007.01.059

7. Muratori M, Tarozzi N, Cambi M, Boni L, Iorio AL, Passaro C, et al. Variation of DNA fragmentation levels during density gradient sperm selection for assisted reproduction techniques: A possible new Male predictive parameter of pregnancy? *Med (Baltimore)* (2016) 95(20):e3624. doi: 10.1097/md.0000000000003624

8. Shirota K, Yotsumoto F, Itoh H, Obama H, Hidaka N, Nakajima K, et al. Separation efficiency of a microfluidic sperm sorter to minimize sperm DNA damage. *Fertil Steril* (2016) 105(2):315–21. doi: 10.1016/j.fertnstert.2015.10.023

9. Quinn MM, Jalalian L, Ribeiro S, Ona K, Demirci U, Cedars MI, et al. Microfluidic sorting selects sperm for clinical use with reduced DNA damage compared to density gradient centrifugation with swim-up in split semen samples. *Hum Reprod* (2018) 33(8):1388–93. doi: 10.1093/humrep/dey239

10. Zhang H, Xuan X, Yang S, Li X, Xu C, Gao X. Selection of viable human spermatozoa with low levels of DNA fragmentation from an immotile population using density gradient centrifugation and magnetic-activated cell sorting. *Andrologia* (2018) 50(1):e12821. doi: 10.1111/and.12821

11. Nasr-Esfahani MH, Deemeh MR, Tavalaee M. New era in sperm selection for ICSI. *Int J Androl* (2012) 35(4):475–84. doi: 10.1111/j.1365-2605.2011.01227.x

12. Sakkas D. Novel technologies for selecting the best sperm for *in vitro* fertilization and intracytoplasmic sperm injection. *Fertil Steril* (2013) 99(4):1023–9. doi: 10.1016/j.fertnstert.2012.12.025

13. Vaughan DA, Sakkas D. Sperm selection methods in the 21st century. *Biol Reprod* (2019) 101(6):1076–82. doi: 10.1093/biolre/ioz032

14. Marzano G, Chiriacò MS, Primiceri E, Dell'Aquila ME, Ramalho-Santos J, Zara V, et al. Sperm selection in assisted reproduction: A review of established methods and cutting-edge possibilities. *Biotechnol Adv* (2020) 40:107498. doi: 10.1016/j.biotechadv.2019.107498

15. Chan PJ, Jacobson JD, Corselli JU, Patton WC. A simple zeta method for sperm selection based on membrane charge. *Fertil Steril* (2006) 85(2):481–6. doi: 10.1016/j.fertnstert.2005.07.1302

16. Gil M, Sar-Shalom V, Melendez Sivira Y, Carreras R, Checa MA. Sperm selection using magnetic activated cell sorting (MACS) in assisted reproduction: a systematic review and meta-analysis. *J Assist Reprod Genet* (2013) 30(4):479–85. doi: 10.1007/s10815-013-9962-8

17. Sakkas D, Ramalingam M, Garrido N, Barratt CL. Sperm selection in natural conception: what can we learn from mother nature to improve assisted reproduction outcomes? *Hum Reprod Update* (2015) 21(6):711–26. doi: 10.1093/humupd/dmv042

18. Yan Y, Zhang B, Fu Q, Wu J, Liu R. A fully integrated biomimetic microfluidic device for evaluation of sperm response to thermotaxis and chemotaxis. *Lab Chip* (2021) 21(2):310–8. doi: 10.1039/d0lc00845a

19. Liu DY, Clarke GN, Martic M, Garrett C, Baker HW. Frequency of disordered zona pellucida (ZP)-induced acrosome reaction in infertile men with normal semen analysis and normal spermatozoa-ZP binding. *Hum Reprod* (2001) 16(6):1185–90. doi: 10.1093/humrep/16.6.1185

20. Liu DY, Baker HW. Frequency of defective sperm-zona pellucida interaction in severely teratozoospermic infertile men. *Hum Reprod* (2003) 18(4):802–7. doi: 10.1093/humrep/deg164

21. Liu DY, Baker HW. High frequency of defective sperm-zona pellucida interaction in oligozoospermic infertile men. *Hum Reprod* (2004) 19(2):228–33. doi: 10.1093/humrep/deh067

22. Liu DY, Liu ML, Garrett C, Baker HW. Comparison of the frequency of defective sperm-zona pellucida (ZP) binding and the ZP-induced acrosome reaction between subfertile men with normal and abnormal semen. *Hum Reprod* (2007) 22(7):1878–84. doi: 10.1093/humrep/dem087

23. Chiu PC, Lam KK, Wong RC, Yeung WS. The identity of zona pellucida receptor on spermatozoa: an unresolved issue in developmental biology. *Semin Cell Dev Biol* (2014) 30:86–95. doi: 10.1016/j.semcdb.2014.04.016

24. Redgrove KA, Anderson AL, Dun MD, McLaughlin EA, O'Bryan MK, Aitken RJ, et al. Involvement of multimeric protein complexes in mediating the capacitation-dependent binding of human spermatozoa to homologous zonae pellucidae. *Dev Biol* (2011) 356(2):460–74. doi: 10.1016/j.ydbio.2011.05.674

25. Liu DY, Garrett C, Baker HW. Low proportions of sperm can bind to the zona pellucida of human oocytes. *Hum Reprod* (2003) 18(11):2382–9. doi: 10.1093/humrep/deg456

26. Liu DY, Stewart T, Baker HW. Normal range and variation of the zona pellucida-induced acrosome reaction in fertile men. *Fertil Steril* (2003) 80(2):384–9. doi: 10.1016/s0015-0282(03)00603-4

27. WHO. *WHO laboratory manual for the examination and processing of human semen. 5th ed*. Geneva: World Health Organization (2011).

28. Chiu PC, Liao S, Lam KK, Tang F, Ho JC, Ho PC, et al. Adrenomedullin regulates sperm motility and oviductal ciliary beat *via* cyclic adenosine 5'-monophosphate/protein kinase a and nitric oxide. *Endocrinology* (2010) 151 (7):3336–47. doi: 10.1210/en.2010-0077

29. Overstreet JW, Hembree WC. Penetration of the zona pellucida of nonliving human oocytes by human spermatozoa *in vitro*. *Fertil Steril* (1976) 27(7):815–31. doi: 10.1016/S0015-0282(16)41959-X

30. Liu DY, Lopata A, Johnston WI, Baker HW. A human sperm-zona pellucida binding test using oocytes that failed to fertilize *in vitro*. *Fertil Steril* (1988) 50(5):782–8. doi: 10.1016/s0015-0282(16)60316-3

31. Bastiaan HS, Windt ML, Menkveld R, Kruger TF, Oehninger S, Franken DR. Relationship between zona pellucida-induced acrosome reaction, sperm morphology, sperm-zona pellucida binding, and *in vitro* fertilization. *Fertil Steril* (2003) 79(1):49–55. doi: 10.1016/s0015-0282(02)04548-x

32. Liu DY, Baker HW. Human sperm bound to the zona pellucida have normal nuclear chromatin as assessed by acridine orange fluorescence. *Hum Reprod* (2007) 22 (6):1597–602. doi: 10.1093/humrep/dem044

33. Liu DY, Liu ML, Clarke GN, Baker HW. Hyperactivation of capacitated human sperm correlates with the zona pellucida-induced acrosome reaction of zona pellucida-bound sperm. *Hum Reprod* (2007) 22(10):2632–8. doi: 10.1093/humrep/dem245

34. Braga DPd.AF, Iaconelli A, Figueira R, d. CS, Madaschi C, Semião-Francisco L, et al. Outcome of ICSI using zona pellucida-bound spermatozoa and conventionally selected spermatozoa. *Reprod BioMed Online* (2009) 19(6):802–7. doi: 10.1016/j.rbmo.2009.09.020

35. Black M, Liu DY, Bourne H, Baker HWG. Comparison of outcomes of conventional intracytoplasmic sperm injection and intracytoplasmic sperm injection using sperm bound to the zona pellucida of immature oocytes. *Fertil Steril* (2010) 93 (2):672–4. doi: 10.1016/j.fertnstert.2009.08.063

36. Liu F, Qiu Y, Zou Y, Deng Z-H, Yang H, Liu DY. Use of zona pellucida–bound sperm for intracytoplasmic sperm injection produces higher embryo quality and implantation than conventional intracytoplasmic sperm injection. *Fertil Steril* (2011) 95(2):815–8. doi: 10.1016/j.fertnstert.2010.09.015

37. Jin R, Bao J, Tang D, Liu F, Wang G, Zhao Y, et al. Outcomes of intracytoplasmic sperm injection using the zona pellucida-bound sperm or manually selected sperm. *J Assist Reprod Genet* (2016) 33(5):597–601. doi: 10.1007/s10815-016-0676-6

38. Yao YQ, Yeung WS, Ho PC. The factors affecting sperm binding to the zona pellucida in the hemizona binding assay. *Hum Reprod* (1996) 11(7):1516–9. doi: 10.1093/oxfordjournals.humrep.a019429

39. Ward CR, Storey BT. Determination of the time course of capacitation in mouse spermatozoa using a chlortetracycline fluorescence assay. *Dev Biol* (1984) 104(2):287–96. doi: 10.1016/0012-1606(84)90084-8

40. Hinrichs K, Love CC, Brinsko SP, Choi YH, Varner DD. *In vitro* fertilization of *in vitro*-matured equine oocytes: effect of maturation medium, duration of maturation, and sperm calcium ionophore treatment, and comparison with rates of fertilization *in vivo* after oviductal transfer. *Biol Reprod* (2002) 67(1):256–62. doi: 10.1095/biolreprod67.1.256

41. Ostermeier GC, Cardona C, Moody MA, Simpson AJ, Mendoza R, Seaman E, et al. Timing of sperm capacitation varies reproducibly among men. *Mol Reprod Dev* (2018) 85(5):387–96. doi: 10.1002/mrd.22972

42. Puga Molina LC, Luque GM, Balestrini PA, Marín-Briggiler CI, Romarowski A, Buffone MG. Molecular basis of human sperm capacitation. *Front Cell Dev Biol* (2018) 6:72. doi: 10.3389/fcell.2018.00072

43. Pang P-C, Chiu PCN, Lee C-L, Chang L-Y, Panico M, Morris HR, et al. Human sperm binding is mediated by the sialyl-lewis(x) oligosaccharide on the zona pellucida. *Science* (2011) 333(6050):1761. doi: 10.1126/science.1207438

44. Chakravarty S, Kadunganattil S, Bansal P, Sharma RK, Gupta SK. Relevance of glycosylation of human zona pellucida glycoproteins for their binding to capacitated human spermatozoa and subsequent induction of acrosomal exocytosis. *Mol Reprod Dev* (2008) 75(1):75–88. doi: 10.1002/mrd.20726

45. Chirinos M, Cariño C, González-González ME, Arreola E, Reveles R, Larrea F. Characterization of human sperm binding to homologous recombinant zona pellucida proteins. *Reprod Sci* (2011) 18(9):876–85. doi: 10.1177/1933719111398146

46. Byrne K, Leahy T, McCulloch R, Colgrave ML, Holland MK. Comprehensive mapping of the bull sperm surface proteome. *Proteomics* (2012) 12(23-24):3559–79. doi: 10.1002/pmic.201200133

47. Wong CW, Lam KKW, Lee CL, Yeung WSB, Zhao WE, Ho PC, et al. The roles of protein disulphide isomerase family a, member 3 (ERp57) and surface thiol/disulphide exchange in human spermatozoa-zona pellucida binding. *Hum Reprod* (2017) 32(4):733–42. doi: 10.1093/humrep/dex007

48. Wang Y, Zhao W, Mei S, Chen P, Leung TY, Lee CL, et al. Identification of sialyl-Lewis(x)-Interacting protein on human spermatozoa. *Front Cell Dev Biol* (2021) 9:700396. doi: 10.3389/fcell.2021.700396

49. Reid AT, Redgrove K, Aitken RJ, Nixon B. Cellular mechanisms regulating sperm-zona pellucida interaction. *Asian J Androl* (2011) 13(1):88–96. doi: 10.1038/aja.2010.74

50. Baker MA, Naumovski N, Hetherington L, Weinberg A, Velkov T, Aitken RJ. Head and flagella subcompartmental proteomic analysis of human spermatozoa. *Proteomics* (2013) 13(1):61–74. doi: 10.1002/pmic.201200350

51. Sabeur K, Cherr GN, Yudin AI, Primakoff P, Li MW, Overstreet JW. The PH-20 protein in human spermatozoa. *J Androl* (1997) 18(2):151–8.

52. Jin M, Fujiwara E, Kakiuchi Y, Okabe M, Satouh Y, Baba SA, et al. Most fertilizing mouse spermatozoa begin their acrosome reaction before contact with the zona pellucida during *in vitro* fertilization. *Proc Natl Acad Sci U.S.A.* (2011) 108 (12):4892–6. doi: 10.1073/pnas.1018202108

53. Harper CV, Cummerson JA, White MR, Publicover SJ, Johnson PM. Dynamic resolution of acrosomal exocytosis in human sperm. *J Cell Sci* (2008) 121(Pt 13):2130–5. doi: 10.1242/jcs.030379

54. Mayer MP, Bukau B. Hsp70 chaperones: cellular functions and molecular mechanism. *Cell Mol Life Sci* (2005) 62(6):670–84. doi: 10.1007/s00018-004-4464-6

55. Son WY, Han CT, Hwang SH, Lee JH, Kim S, Kim YC. Repression of hspA2 messenger RNA in human testes with abnormal spermatogenesis. *Fertil Steril* (2000) 73 (6):1138–44. doi: 10.1016/s0015-0282(00)00496-9

56. Lima SB, Cenedeze MA, Bertolla RP, Filho PA, Oehninger S, Cedenho AP. Expression of the HSPA2 gene in ejaculated spermatozoa from adolescents with and without varicocele. *Fertil Steril* (2006) 86(6):1659–63. doi: 10.1016/j.fertnstert.2006.05.030

57. Cedenho AP, Lima SB, Cenedeze MA, Spaine DM, Ortiz V, Oehninger S. Oligozoospermia and heat-shock protein expression in ejaculated spermatozoa. *Hum Reprod* (2006) 21(7):1791–4. doi: 10.1093/humrep/del055

58. Huszar G, Stone K, Dix D, Vigue L. Putative creatine kinase m-isoform in human sperm is identifiedas the 70-kilodalton heat shock protein HspA2. *Biol Reprod* (2000) 63(3):925–32. doi: 10.1095/biolreprod63.3.925

59. Huszar G, Ozenci CC, Cayli S, Zavaczki Z, Hansch E, Vigue L. Hyaluronic acid binding by human sperm indicates cellular maturity, viability, and unreacted acrosomal status. *Fertil Steril* (2003) 79:1616–24. doi: 10.1016/s0015-0282(03)00402-3

60. Huszar G, Ozkavukcu S, Jakab A, Celik-Ozenci C, Sati GL, Cayli S. Hyaluronic acid binding ability of human sperm reflects cellular maturity and fertilizing potential:

selection of sperm for intracytoplasmic sperm injection. *Curr Opin Obstet Gynecol* (2006) 18(3):260–7. doi: 10.1097/01.gco.0000193018.98061.2f

61. Ergur AR, Dokras A, Giraldo JL, Habana A, Kovanci E, Huszar G. Sperm maturity and treatment choice of *in vitro* fertilization (IVF) or intracytoplasmic sperm injection: diminished sperm HspA2 chaperone levels predict IVF failure. *Fertil Steril* (2002) 77(5):910–8. doi: 10.1016/s0015-0282(02)03073-x

62. Motiei M, Tavalaee M, Rabiei F, Hajihosseini R, Nasr-Esfahani MH. Evaluation of HSPA2 in fertile and infertile individuals. *Andrologia* (2013) 45(1):66–72. doi: 10.1111/j.1439-0272.2012.01315.x

63. Heidari M, Darbani S, Darbandi M, Lakpour N, Fathi Z, Zarnani AH, et al. Assessing the potential of HSPA2 and ADAM2 as two biomarkers for human sperm selection. *Hum Fertil (Camb)* (2020) 23(2):123–33. doi: 10.1080/14647273.2018.1534277

64. Redgrove KA, Nixon B, Baker MA, Hetherington L, Baker G, Liu DY, et al. The molecular chaperone HSPA2 plays a key role in regulating the expression of sperm surface receptors that mediate sperm-egg recognition. *PloS One* (2012) 7(11):e50851. doi: 10.1371/journal.pone.0050851

65. Redgrove KA, Anderson AL, McLaughlin EA, Bryan MK, Aitken RJ, Nixon B. Investigation of the mechanisms by which the molecular chaperone HSPA2 regulates the expression of sperm surface receptors involved in human sperm-oocyte recognition. *Mol Hum Reprod* (2013) 19(3):120–35. doi: 10.1093/molehr/gas064

66. Gómez-Torres MJ, Huerta-Retamal N, Robles-Gómez L, Sáez-Espinosa P, Aizpurua J, Avilés M, et al. Arylsulfatase a remodeling during human sperm *In vitro* capacitation using field emission scanning electron microscopy (FE-SEM). *Cells* (2021) 10(2):222. doi: 10.3390/cells10020222

67. Huerta-Retamal N, Sáez-Espinosa P, Robles-Gómez L, Avilés M, Romero A, Aizpurua J, et al. Human sperm chaperone HSPA2 distribution during *in vitro* capacitation. *J Reprod Immunol* (2021) 143:103246. doi: 10.1016/j.jri.2020.103246

68. Mandal A, Klotz KL, Shetty J, Jayes FL, Wolkowicz MJ, Bolling LC, et al. SLLP1, a unique, intra-acrosomal, non-bacteriolytic, c lysozyme-like protein of human spermatozoa. *Biol Reprod* (2003) 68(5):1525–37. doi: 10.1095/biolreprod.102.010108

69. Zheng H, Mandal A, Shumilin IA, Chordia MD, Panneerdoss S, Herr JC, et al. Sperm lysozyme-like protein 1 (SLLP1), an intra-acrosomal oolemmal-binding sperm protein, reveals filamentous organization in protein crystal form. *Andrology* (2015) 3(4):756–71. doi: 10.1111/andr.12057

70. Herrero MB, Mandal A, Digilio LC, Coonrod SA, Maier B, Herr JC. Mouse SLLP1, a sperm lysozyme-like protein involved in sperm-egg binding and fertilization. *Dev Biol* (2005) 284(1):126–42. doi: 10.1016/j.ydbio.2005.05.008

71. Wassarman PM. Zona pellucida glycoproteins. *Annu Rev Biochem* (1988) 57:415–42. doi: 10.1146/annurev.bi.57.070188.002215

72. Sinowatz F, Töpfer-Petersen E, Kölle S, Palma G. Functional morphology of the zona pellucida. *Anat Histol Embryol* (2001) 30(5):257–63. doi: 10.1046/j.1439-0264.2001.00337.x

73. Jiménez-Movilla M, Avilés M, Gómez-Torres MJ, Fernández-Colom PJ, Castells MT, de Juan J, et al. Carbohydrate analysis of the zona pellucida and cortical granules of human oocytes by means of ultrastructural cytochemistry. *Hum Reprod* (2004) 19(8):1842–55. doi: 10.1093/humrep/deh311

74. Miranda PV, Gonzalez-Echeverría F, Marín-Briggiler CI, Brandelli A, Blaquier JA, Tezón JG. Glycosidic residues involved in human sperm-zona pellucida binding *in vitro*. *Mol Hum Reprod* (1997) 3(5):399–404. doi: 10.1093/molehr/3.5.399

75. Miranda PV, González-Echeverría F, Blaquier JA, Mahuran DJ, Tezón JG. Evidence for the participation of beta-hexosaminidase in human sperm-zona pellucida interaction *in vitro*. *Mol Hum Reprod* (2000) 6(8):699–706. doi: 10.1093/molehr/6.8.699

76. Zitta K, Wertheimer E, Miranda PV. Analysis of the participation of n-acetylglucosamine in the different steps of sperm-zona pellucida interaction in hamster. *Mol Hum Reprod* (2004) 10(12):925–33. doi: 10.1093/molehr/gah122

77. Petit FM, Serres C, Bourgeon F, Pineau C, Auer J. Identification of sperm head proteins involved in zona pellucida binding. *Hum Reprod* (2013) 28(4):852–65. doi: 10.1093/humrep/des452

78. Panner Selvam MK, Ambar RF, Agarwal A, Henkel R. Etiologies of sperm DNA damage and its impact on male infertility. *Andrologia* (2021) 53(1):e13706. doi: 10.1111/and.13706

79. Ford WC. Regulation of sperm function by reactive oxygen species. *Hum Reprod Update* (2004) 10(5):387–99. doi: 10.1093/humupd/dmh034

80. Aitken RJ, Baker MA. The role of genetics and oxidative stress in the etiology of Male infertility-a unifying hypothesis? *Front Endocrinol (Lausanne)* (2020) 11:581838. doi: 10.3389/fendo.2020.581838

81. Tesarik J. Late, but not early, paternal effect on human embryo development is related to sperm DNA fragmentation. *Hum Reprod* (2004) 19(3):611–5. doi: 10.1093/humrep/deh127

82. Twigg JP, Irvine DS, Aitken RJ. Oxidative damage to DNA in human spermatozoa does not preclude pronucleus formation at intracytoplasmic sperm injection. *Hum Reprod* (1998) 13(7):1864–71. doi: 10.1093/humrep/13.7.1864

83. Zini A, Meriano J, Kader K, Jarvi K, Laskin CA, Cadesky K. Potential adverse effect of sperm DNA damage on embryo quality after ICSI. *Hum Reprod* (2005) 20(12):3476–80. doi: 10.1093/humrep/dei266

84. Zhao J, Zhang Q, Wang Y, Li Y. Whether sperm deoxyribonucleic acid fragmentation has an effect on pregnancy and miscarriage after *in vitro* fertilization/intracytoplasmic sperm injection: a systematic review and meta-analysis. *Fertil Steril* (2014) 102(4):998–1005.e1008. doi: 10.1016/j.fertnstert.2014.06.033

85. Osman A, Alsomait H, Seshadri S, El-Toukhy T, Khalaf Y. The effect of sperm DNA fragmentation on live birth rate after IVF or ICSI: a systematic review and meta-analysis. *Reprod BioMed Online* (2015) 30(2):120–7. doi: 10.1016/j.rbmo.2014.10.018

86. Simon L, Liu L, Murphy K, Ge S, Hotaling J, Aston KI, et al. Comparative analysis of three sperm DNA damage assays and sperm nuclear protein content in couples undergoing assisted reproduction treatment. *Hum Reprod* (2014) 29(5):904–17. doi: 10.1093/humrep/deu040

87. Sharma R, Masaki J, Agarwal A. Sperm DNA fragmentation analysis using the TUNEL assay. *Methods Mol Biol* (2013) 927:121–36. doi: 10.1007/978-1-62703-038-0_12

88. Cohen-Bacrie P, Belloc S, Ménézo YJ, Clement P, Hamidi J, Benkhalifa M. Correlation between DNA damage and sperm parameters: a prospective study of 1,633 patients. *Fertil Steril* (2009) 91(5):1801–5. doi: 10.1016/j.fertnstert.2008.01.086

89. Nijs M, De Jonge C, Cox A, Janssen M, Bosmans E, Ombelet W. Correlation between male age, WHO sperm parameters, DNA fragmentation, chromatin packaging and outcome in assisted reproduction technology. *Andrologia* (2011) 43(3):174–9. doi: 10.1111/j.1439-0272.2010.01040.x

90. Tejada RI, Mitchell JC, Norman A, Marik JJ, Friedman S. A test for the practical evaluation of male fertility by acridine orange (AO) fluorescence. *Fertil Steril* (1984) 42(1):87–91. doi: 10.1016/s0015-0282(16)47963-x

91. Eggert-Kruse W, Rohr G, Kerbel H, Schwalbach B, Demirakca T, Klinga K, et al. The acridine orange test: a clinically relevant screening method for sperm quality during infertility investigation? *Hum Reprod* (1996) 11(4):784–9. doi: 10.1093/oxfordjournals.humrep.a019255

92. Georgiou I, Syrrou M, Pardalidis N, Karakitsios K, Mantzavinos T, Giotitsas N, et al. Genetic and epigenetic risks of intracytoplasmic sperm injection method. *Asian J Androl* (2006) 8(6):643–73. doi: 10.1111/j.1745-7262.2006.00231.x

93. Sharma R, Agarwal A, Rohra VK, Assidi M, Abu-Elmagd M, Turki RF. Effects of increased paternal age on sperm quality, reproductive outcome and associated epigenetic risks to offspring. *Reprod Biol Endocrinol* (2015) 13:35. doi: 10.1186/s12958-015-0028-x

94. Donkin I, Barrès R. Sperm epigenetics and influence of environmental factors. *Mol Metab* (2018) 14:1–11. doi: 10.1016/j.molmet.2018.02.006

95. Åsenius F, Danson AF, Marzi SJ. DNA Methylation in human sperm: a systematic review. *Hum Reprod Update* (2020) 26(6):841–73. doi: 10.1093/humupd/dmaa025

96. de Yebra L, Ballescá JL, Vanrell JA, Corzett M, Balhorn R, Oliva R. Detection of P2 precursors in the sperm cells of infertile patients who have reduced protamine P2 levels. *Fertil Steril* (1998) 69(4):755–9. doi: 10.1016/s0015-0282(98)00012-0

97. Aoki VW, Liu L, Jones KP, Hatasaka HH, Gibson M, Peterson CM, et al. Sperm protamine 1/protamine 2 ratios are related to *in vitro* fertilization pregnancy rates and predictive of fertilization ability. *Fertil Steril* (2006) 86(5):1408–15. doi: 10.1016/j.fertnstert.2006.04.024

98. Oliva R. Protamines and male infertility. *Hum Reprod Update* (2006) 12(4):417–35. doi: 10.1093/humupd/dml009

99. Nanassy L, Liu L, Griffin J, Carrell DT. The clinical utility of the protamine 1/protamine 2 ratio in sperm. *Protein Pept Lett* (2011) 18(8):772–7. doi: 10.2174/092986611795713934

100. Boissonnas CC, Abdalaoui HE, Haelewyn V, Fauque P, Dupont JM, Gut I, et al. Specific epigenetic alterations of IGF2-H19 locus in spermatozoa from infertile men. *Eur J Hum Genet* (2010) 18(1):73–80. doi: 10.1038/ejhg.2009.117

101. Hammoud SS, Purwar J, Pflueger C, Cairns BR, Carrell DT. Alterations in sperm DNA methylation patterns at imprinted loci in two classes of infertility. *Fertil Steril* (2010) 94(5):1728–33. doi: 10.1016/j.fertnstert.2009.09.010

102. Cui X, Jing X, Wu X, Yan M, Li Q, Shen Y, et al. DNA Methylation in spermatogenesis and male infertility. *Exp Ther Med* (2016) 12(4):1973–9. doi: 10.3892/etm.2016.3569

103. Santi D, De Vincentis S, Magnani E, Spaggiari G. Impairment of sperm DNA methylation in male infertility: a meta-analytic study. *Andrology* (2017) 5(4):695–703. doi: 10.1111/andr.12379

104. Bahreinian M, Tavalaee M, Abbasi H, Kiani-Esfahani A, Shiravi AH, Nasr-Esfahani MH. DNA Hypomethylation predisposes sperm to DNA damage in individuals with varicocele. *Syst Biol Reprod Med* (2015) 61(4):179–86. doi: 10.3109/19396368.2015.1020116

105. Montjean D, Zini A, Ravel C, Belloc S, Dalleac A, Copin H, et al. Sperm global DNA methylation level: association with semen parameters and genome integrity. *Andrology* (2015) 3(2):235–40. doi: 10.1111/andr.12001

106. Santana VP, James ER, Miranda-Furtado CL, Souza MF, Pompeu CP, Esteves SC, et al. Differential DNA methylation pattern and sperm quality in men with varicocele. *Fertil Steril* (2020) 114(4):770–8. doi: 10.1016/j.fertnstert.2020.04.045

107. Rahiminia T, Yazd EF, Fesahat F, Moein MR, Mirjalili AM, Talebi AR. Sperm chromatin and DNA integrity, methyltransferase mRNA levels, and global DNA methylation in oligoasthenoteratozoospermia. *Clin Exp Reprod Med* (2018) 45(1):17–24. doi: 10.5653/cerm.2018.45.1.17

108. Laqqan M, Ahmed I, Yasin M, Hammadeh ME, Yassin M. Influence of variation in global sperm DNA methylation level on the expression level of protamine genes and human semen parameters. *Andrologia* (2020) 52(1):e13484. doi: 10.1111/and.13484

109. Clark SJ, Smallwood SA, Lee HJ, Krueger F, Reik W, Kelsey G. Genome-wide base-resolution mapping of DNA methylation in single cells using single-cell bisulfite sequencing (scBS-seq). *Nat Protoc* (2017) 12(3):534–47. doi: 10.1038/nprot.2016.187

110. Wang L, Chen M, Yan G, Zhao S. DNA Methylation differences between zona pellucida-bound and manually selected spermatozoa are associated with autism susceptibility. *Front Endocrinol (Lausanne)* (2021) 12:774260. doi: 10.3389/fendo.2021.774260

111. McCallum C, Riordon J, Wang Y, Kong T, You JB, Sanner S, et al. Deep learning-based selection of human sperm with high DNA integrity. *Commun Biol* (2019) 2(1):250–10. doi: 10.1038/s42003-019-0491-6

112. Anbari F, Khalili MA, Sultan Ahamed AM, Mangoli E, Nabi A, Dehghanpour F. Sabour M. Microfluidic sperm selection yields higher sperm quality compared to conventional method in ICSI program: A pilot study. *Syst Biol Reprod Med* (2021) 67 (2):137–43. doi: 10.1080/19396368.2020.1837994